

Received Date : 02-May-2016

Revised Date : 24-Jun-2016

Accepted Date : 05-Jul-2016

Article type : Standard Papers

Editor : Jason Rohr

## **Mollusc-shell debris can mitigate the deleterious effects of organic pollution on marine sediments**

*Nuria Casado-Coy\*, Elena Martinez-Garcia, Pablo Sanchez-Jerez, Carlos Sanz-Lazaro*

Departamento de Ciencias del Mar y Biología Aplicada, Universidad de Alicante, PO Box 99, E-03080 Alicante, Spain.

\* Corresponding author: [ncasadocoy@ua.es](mailto:ncasadocoy@ua.es)

E-mail of the rest of the authors: [elena.martinez@ua.es](mailto:elena.martinez@ua.es), [psanchez@ua.es](mailto:psanchez@ua.es), [carsanz@ua.es](mailto:carsanz@ua.es)

\*Corresponding author

**Running Title:** Mollusc debris mitigates organic pollution.

This article has been accepted for publication and undergone full peer review but has not been through the copyediting, typesetting, pagination and proofreading process, which may lead to differences between this version and the Version of Record. Please cite this article as doi: 10.1111/1365-2664.12748

This article is protected by copyright. All rights reserved.

Accepted Article

## Summary

1. Organic pollution is widespread in coastal areas and can have profound impacts on the seabed. Coastal sediments play an important role at a global scale in the recycling of organic matter, and this process is influenced by the habitat complexity of the sediments, among other factors. Mollusc shells are produced as a waste product from a range of anthropogenic activities, but we demonstrate that they can be used to increase the habitat complexity of sediments.

2. We studied the effect of mussel-shell debris (shell-hash) on the biogeochemical processes of marine sediments affected by organic pollution, using a mesocosm experiment simulating the bioturbation effects of macrofauna.

3. We found that shell-hash improved the ecological status of organically-polluted sediments by reducing the accumulation of sulphide from anaerobic metabolic pathways.

4. Additionally, when shell-hash was present in an organically-polluted sediment, there was a decrease in ammonium release to the water column, thus preventing the negative ecological consequences of eutrophication.

5. *Synthesis and applications.* Our study indicates that shell-hash debris can be used as a potential tool to mitigate the effects of organic enrichment on marine sediments. A density of shell-hash debris of  $1900 \text{ g m}^{-2}$  in the sediment can diminish toxic by-products (sulphides and ammonium) derived from the stimulation of anaerobic metabolic pathways by organic pollution, at levels that are biologically relevant. The

mitigation effect of shell-hash is more pronounced in sediments where macrofauna is not present.

**Key-words:** aquaculture, biogeochemical fluxes, eutrophication, habitat complexity, pollution mitigation, organic enrichment, sediment metabolism, shell-hash, waste management, waste reuse

## **Introduction**

Marine sediments act as a major sink of organic matter (OM), and have an important role in the cycling of nutrients at a global scale (Duarte, Middelburg & Caraco 2005). This function is especially important in coastal sediments, which are responsible for more than half of the mineralisation of the total OM that accumulates in the seabed (John I. Hedge 1995). Coastal areas are highly exposed to pollution because they are often densely populated. Organic pollution, which is the excess of organic matter above natural deposition rates, is one of the most widespread forms of pollution worldwide (Islam & Tanaka 2004). It can be caused by a range of anthropogenic activities such as agriculture, aquaculture and discharges of sewage (Cloern 2001; Newell 2004; Sanz-Lázaro & Marín 2008).

Bacteria play the most important role in the mineralisation of OM in sediments (Duarte, Middelburg & Caraco 2005), through a variety of metabolic pathways. Their metabolic capacity depends on their electron-acceptor availability. Benthic fauna, through the active movement of particles (bioirrigation) and solutes (bioturbation) improve electron-acceptor supply from the water column, enhancing the metabolic capacity of the sediment (Aller & Aller 1998; Meysman, Middelburg & Heip 2006). Aerobic respiration is the most efficient metabolic pathway, and as oxygen becomes exhausted, there is a sequential consumption of other electron acceptors from higher to

lower efficiency (Holmer & Barry 2005). Sulphate reduction is the most important anaerobic metabolic pathway, which can account for up to half of the total benthic metabolism (Jørgensen 1982). When all electron acceptors have been consumed, methanogenesis occurs through the fermentation of the OM.

Augmenting inputs of OM causes an increase in sediment metabolism, and thus oxygen consumption, preventing its accumulation. Excessive loads of OM can lead to hypoxic or even anoxic conditions, favouring anaerobic metabolic pathways over aerobic ones (Welsh & Castadelli 2004). This situation leads to a decrease in the sediment's metabolic capacity, slowing the rate of OM mineralisation. Additionally, anaerobic pathways produce a series of toxic by-products, such as sulphides and methane (Holmer, Duarte & Marbá 2005; Valdemarsen, Kristensen & Holmer 2010). Oxygen depletion, together with a high concentration of these toxic by-products, can have negative impacts on benthic communities and can cause the defaunation of the sediment (Pearson & Rosenberg 1978; Gray, Wu & Or 2002; Hargrave, Holmer & Newcombe 2008). This can decrease the electron-acceptor supply in the sediment, and consequently, its metabolic capacity (Sanz-Lázaro *et al.* 2011).

Under oxic conditions, the mineralisation product of phosphorous ( $\text{PO}_4^{3-}$ ) is retained in the sediment, bound to iron hydroxides. When conditions are hypoxic, sulphides bind to the iron, causing  $\text{PO}_4^{3-}$  to be released into the water column (McManus 1997). In the case of nitrogen ( $\text{N}_2$ ), under hypoxic conditions, the decoupling of the nitrification-denitrification process causes a reduction in  $\text{N}_2$  production. Therefore, the production of molecules at intermediate steps of the mineralisation of nitrogen (such as  $\text{NH}_4^+$ ,  $\text{NO}_3^-$  and  $\text{NO}_2^-$ ) is increased (Stief 2013). Overall, hypoxic conditions in the sediment promote the release of inorganic nutrients to the water column (Sanz-Lazaro, Valdemarsen & Holmer 2015), which can combine

with other sources of pollution and cause eutrophication, resulting in negative ecological consequences such as algal blooms (Gray, Wu & Or 2002).

Marine sediments are influenced by a range of environmental parameters, including changes in water flow, resource transport, sessile organism attachment availability, and sediment grain size (Sebens 1991). Habitat complexity modulates these parameters, and, consequently, increases in the heterogeneity of the sediment, can enhance its functions, such as benthic metabolism. The shells of molluscs in various states of decomposition (referred to as 'shell-hash'; Wilding 2012) are important elements of the habitat structure that promote its complexity, by modifying grain size and augmenting sessile organism attachment (Gutierrez *et al.* 2003). Large volumes of shell-hash are obtained as a residue from different activities such as aquaculture and the canning industry (Barros *et al.* 2009). This residue could be recovered to increase the habitat complexity of sediments, and therefore to improve the ecological status of the sediment, due to an enhanced metabolic capacity (Dolmer & Frandsen 2002).

To test this hypothesis, we study the effect of shell-hash on the biogeochemistry of marine sediments affected by organic pollution. We carried out a mesocosm experiment to test whether shell-hash could ameliorate the ecological status of organically-polluted sediments, and whether these effects could complement those of macrofauna.

## **Materials and methods**

### *Sampling of sediment and polychaete worms*

The sediment used for the experiment was collected at The Gola beach, Santa Pola, Spain (38°11'18.81"N 0°35'34.55"O). It was a carbonated sediment typical of the Mediterranean. It was graded as a very fine and fine sand grain (0.063-0.25 mm)

according to the Wentworth (1922) classification. A volume of 30 litres of sediment was collected at a 0-10 cm depth range with a shovel, and was sieved through a 0.5 mm mesh to remove the existing macrofauna. To simulate the effect of macrofauna we introduced the polychaete *Lumbrineris latreilli* Audouin & Milne Edwards, 1834, which was collected at the beach of Torrevieja, Spain (38 ° 1'14.38 "N 0 ° 39'8.40" W) in August 2014.

#### *Experimental setup*

Sodium sulphate (50 mmol L<sup>-1</sup>) was added to the sediment and homogenized manually to prevent sulphate depletion during sediment incubation. A total of 36 methacrylate cores (with an internal diameter of 6 cm and a length of 32 cm) were filled with sediment to a depth of 20 cm. The bottom of the cores was sealed with a rubber stopper, leaving ~12 cm of water above the sediment. The cores were left to stratify for 4 days, and were then distributed into 2 groups: a control with unenriched sediment (-OM) and an organically enriched sediment (+OM). The surface of the sediment of +OM cores was enriched with 5.62 g of the same sediment containing 92 g of labile OM per kg of sediment in the form of finely ground fish feed [L-4 Alternate CMX 20 2P BB2, SKRETTING (46.5% protein, 20% fats and oils, 6.1% minerals, fiber 2.2%, 1% phosphorus, 0.9% calcium and 0.4% sodium)]. This enrichment was performed once a week during the experiment. The organic enrichment in +OM cores was 0.1 mmol POC cm<sup>-3</sup> sediment. This level has proved optimal for the stimulation of microbial metabolism in previous enrichment studies (Valdemarsen, Kristensen & Holmer 2010) and corresponds to a realistic OM input to sediments that are subject to organic enrichment in natural environments, such as the sediments underlying fish or mussel

farms (Morrisey *et al.* 2000; Callier *et al.* 2006; Holmer *et al.* 2007; Sanz-Lazaro *et al.* 2011).

We produced shell-hash using shells of the mussel *Mytilus galloprovincialis* Lamarck, 1819. We removed the epibiotic remnants from the outer surface of the shells by gently rubbing them with a scourer, and then broke the valves into fragments (4-5 cm length, 2-3 cm width). We added *c.* 5.4 grams of shell-hash per core, which corresponded to a density of *c.* 1900 g m<sup>-2</sup> (Wilding 2012). Shell hash was placed in the cores at two depth levels: 1) on the sediment surface (+MS), simulating an initial deposition of shell-hash, and 2) half-buried (+MB) (pressed 3-4 cm vertically into the sediment), simulating shell-hash deposited for a longer time. The area of sediment in the cores occupied by shell-hash was between 50 and 70% for +MS cores, and between 10 and 30% for +MB cores (see Fig. S1 in Supporting Information). An additional control treatment without shell-hash fragments (-M) was included. The factor 'shell-hash' was considered as a fixed factor, with three levels. After the 4 days that the sediment of the cores was left for stratification, the shell-hash fragments were added.

To simulate the bioirrigation of macrofauna in natural sediments, three healthy worms (*L. latreilli*) of 14 - 20 cm length were added to each core (*c.* 1300 individuals m<sup>-2</sup>), simulating the natural density observed in the location where they were collected (Casado-Coy and Sanz-Lázaro pers. obs.). 18 cores contained worms (+W), while the other 18 were worm-free controls (-W). Worms were added seven days after the addition of the shell-hash and OM. At this point, we considered that the experiment had started.

Cores were maintained at 16°C in a tank containing 75 L seawater from The Gola beach with a salinity of 37.6. The seawater was filtered to remove large particles (Whatman GF/F Glass Microfiber Filters, 0.7µm, 4.7cm; 100/Box, USA). The water

tank was vigorously oxygenated by air pumps, using the incubation system proposed by Piedecausa *et al.* (2012). The water above the sediment cores was circulated by magnetic bars (4 cm length) placed a few centimetres above the sediment surface, and driven by a rotating magnet (60 rpm) placed close to the cores. The temperature was controlled by two coolers that recirculated the water through the tank, and was monitored several times per day. The cores were kept submerged and in darkness throughout the experiment. More than half of the volume of the tank was exchanged with fresh seawater every 1-2 days to prevent accumulation or depletion of metabolites.

#### *TCO<sub>2</sub> and SOU fluxes*

Total CO<sub>2</sub> (TCO<sub>2</sub>), sediment oxygen uptake (SOU) and nutrient fluxes were determined by the integration of seven incubations performed during the time span of the experiment. Initially, they were performed every 2 or 3 days during the first two weeks, and once per week thereafter. The incubations were performed by sealing the upper part of the core with a rubber stopper for specific time periods (2-4 hours for +OM and 4-5 hours for -OM cores) aiming to prevent O<sub>2</sub> depletion below 60% of the initial concentration in the water column (Glud 2008). At the beginning and at the end of the incubation water samples were taken to calculate consumption/production rates from the difference between these measurements. The O<sub>2</sub> samples were measured with an oximeter and the TCO<sub>2</sub> was measured using a total Carbon titration with titrasol HCl (0.1 mol L<sup>-1</sup>, Applichem Panreac, Germany Methyl Red. Verify periodically the titer) at two pH ranges (Gran *et al.* 1950).

#### *Nutrients*

The water used to determine nutrients was initially filtered with an MCE Syringe (Syringe Filter - 13mm 0.22um CA-CN with Luer lock, 100/pk United Kingdom) filter (Ø 0.22 µm), transferred to 15 mL plastic vials, and frozen (-20 °C) until analysis. The



Accepted Article

nutrients ( $\text{NH}_4^+$ ,  $\text{PO}_4^{3-}$ ,  $\text{NO}_2^-$  and  $\text{NO}_3^-$ ) were analysed using an Automated Wet Chemistry Analyser - Continuous Flow Analyser (Breda, the Netherlands). Fluxes were integrated for the duration of the experiment and reported as  $\text{mmol m}^{-2} \text{d}^{-1}$ .

#### *Sectioning of cores*

2 - 3 days after the last incubation, the cores were sectioned in 1 cm intervals from 0 to 2 cm, and in 2 cm intervals from 2 to 16 cm, in order to measure porewater and analyse the sediment. The cores were sliced after removing the shell-hash, keeping the space occupied by it, so that density values included the effect of the shell-hash. For the AVS analysis, 5ml of sediment was frozen in plastic bags, taking special care to prevent air bubble formation, while for sediment density we used 2 ml.

#### *Sediment analyses*

The irrigation rates of *L. latreilli* were estimated according to Heilskov, Alperin & Holmer (2006). One day prior to the final sectioning of the cores, the water portion of each core was enriched with bromine ( $\text{Br}^-$ ) to a final concentration of *c.* 8 mmol/L. After 24 hours, the cores were sectioned and the porewater of the sediment in each section was extracted by a filter system powered by a vacuum pump. Samples were kept at 4 °C until analysis by ion-chromatography with a Dionex auto-suppressed anion-system, IonPac AS9-HC column and AG9-HC suppressor (Thermo Fisher Scientific, Sunnyvale, USA.) and bicarbonate/carbonate eluent. Bioirrigation was quantified by modelling the excess bromide distribution in the porewater at the end of the incubation. Irrigation activity was calculated from the depth-integrated  $\text{Br}^-$  inventory and corrected for the effects of passive diffusion.

Sediment density was determined as the weight of a known volume, while water content was measured as the weight difference after desiccation. Total OM was determined by weight loss upon ignition for 4 h at 450 °C. The value of OM for the integrated treatment was calculated as a percentage of each section, obtaining one value for each core. The sediment for measuring the mmol m<sup>-2</sup> of the AVS accumulated in the sediment was fixed by freezing in plastics bags. Prior to analysis, sediment was thawed. AVS samples were distilled and quantified following the methodology proposed by Allen, Fu & Deng (1993).

#### *Experimental design and data analysis*

The measured variables were compared among treatments using a three-way ANOVA, where the fixed factors were: *organic pollution* (with two treatments, with and without organic enrichment, -OM and +OM), *worms* (with two treatments, with and without worms, +W and -W) and *shell-hash* (with three treatments, no shell-hash, with shell-hash on the sediment surface, and with shell-hash buried in the sediment, -M, +MS and +MB, respectively). Before carrying out the ANOVA, normality and homogeneity of variance was checked using Cochran's test and p-p plots (Underwood 1997). If assumptions were violated, transformations were applied and assumptions were re-checked. If the differences between interactions of any of the three factors were significant, the Student-Newman-Keuls *post-hoc* test for multiple comparisons was applied. To assess whether significant differences were biologically relevant, we calculated the effect size (Nakagawa & Cuthill 2007). All statistical tests were conducted with a significance level of  $\alpha=0.05$ . Data were reported as mean  $\pm$  standard error (SE), while the size of effect was reported with the 95% confidence interval (CI).

## Results

### *TCO<sub>2</sub>*

TCO<sub>2</sub> fluxes ranged from 22.3±16.4 to 294.4±42.0 mmol m<sup>-2</sup> d<sup>-1</sup>. The increasing trends over time levelled off at the end, except for +OM–M–W cores, where the increasing trend was maintained for the whole experiment (see Fig. S3). Time-integrated TCO<sub>2</sub> fluxes showed significant interactions among all the factors (see Table S1) (Fig. 1). +OM–W cores with *shell-hash* (+MS and +MB) had an effect decreasing the TCO<sub>2</sub> flux by 148.1 with a CI of 42.2 to 253.9 mmol m<sup>-2</sup> d<sup>-1</sup> compared to cores without *shell-hash* (-M). When *worms* were present (+W), the effect of *shell-hash* was not biologically relevant in +OM cores, decreasing the TCO<sub>2</sub> flux by only 1.9 with a CI of 75.9 to -79.8 mmol m<sup>-2</sup> d<sup>-1</sup>. The effect of *shell-hash* separated when being on surface (+MS) than when buried (+MB) under *organic pollution* conditions is shown in Fig. 2.

### *Sediment Oxygen Uptake*

SOU values ranged from 24.0±4.9 to 75.1±3.6 mmol m<sup>-2</sup> d<sup>-1</sup>. The increasing trends over time levelled off in the -OM cores at the end, but in the +OM cores the range was greater (see Fig. S3). In time-integrated SOU values, the factor with the greatest effect was *organic pollution* (33.4 mmol m<sup>-2</sup> d<sup>-1</sup> with a CI of 22.1 to 44.6) (Fig. 1). Time-integrated SOU values showed a significant interaction between OM and M (see Table S1). *Shell-hash* on the sediment surface (+MS) in +OM -W cores had an effect of lowering SOU by 40.1 with a CI of 51.2 to 29.1 mmol m<sup>-2</sup> d<sup>-1</sup>. Under *organic pollution* when *worms* were present (+OM +W), the effect size of *shell-hash* was not biologically relevant (5.7 with a CI of -45.0 to 33.6 mmol m<sup>-2</sup> d<sup>-1</sup>) (Fig. 1).

### *TCO<sub>2</sub>:O<sub>2</sub> ratio*

Time-integrated  $\text{TCO}_2:\text{O}_2$  values showed significant interactions among all the factors (see Table S1) (Fig. 1). *Shell-hash* buried in the sediment (+MB) in +OM–W cores had an effect decreasing the  $\text{TCO}_2:\text{O}_2$  ratio by 1.9 with a CI of 4.4 to -0.5. When *worms* were present (+W), the effect size of *shell-hash* (+MS and +MB) was not biological relevant (0.1 with a CI of -0.4 to 0.6).

#### *Nitrogen compounds*

$\text{NH}_4^+$  fluxes ranged from  $5.8 \pm 1.0$  to  $25.5 \pm 2.0$   $\text{mmol m}^{-2} \text{d}^{-1}$ . The increasing trends over time levelled off at the end, except for +OM–W–M cores, where the increasing trend was maintained throughout the experiment (see Fig. S4). The trends of time-integrated  $\text{NH}_4^+$  fluxes were very similar to those obtained in  $\text{TCO}_2$  fluxes (Fig. 3). Time-integrated  $\text{NH}_4^+$  fluxes showed a significant interaction between OM and M, on the one hand, and between W and M, on the other (Table 1). The  $\text{NH}_4^+$  fluxes of the +OM–W cores containing *shell-hash* were nearly half those of the cores without *shell-hash* (-M) (Fig. 3). *Shell-hash* in +OM–W cores had an effect decreasing the  $\text{NH}_4^+$  fluxes by 11.4 with a CI of 5.4 to 17.5  $\text{mmol m}^{-2} \text{d}^{-1}$ . When *worms* were present (+W), the effect size of *shell-hash* (+MS and +MB together) was not biologically relevant 0.6 with a CI of -6.4 to -7.6  $\text{mmol m}^{-2} \text{d}^{-1}$ . The effect of *Shell-hash* separated when being in surface (+MS) than when buried (+MB) under *organic pollution* conditions and without *worms* is shown in Fig. 2.

$\text{NO}_2^-$  fluxes ranged from  $-0.12 \pm 0.10$  to  $0.04 \pm 0.04$   $\text{mmol m}^{-2} \text{d}^{-1}$ . In general, the trends were negative in the +OM cores and stable in the -OM cores (see Fig. S4). In -OM cores time-integrated  $\text{NO}_2^-$  fluxes were close to 0 (Fig. 3), and significantly higher than +OM cores (Table 1). *Organic pollution* had an effect of decreasing the  $\text{NO}_2^-$  fluxes by 4.9 with a CI of 2.0 to 7.8  $\text{mmol m}^{-2} \text{d}^{-1}$ .

Accepted Article

$\text{NO}_3^-$  fluxes ranged from  $0.06 \pm 0.09$  to  $0.20 \pm 0.05$   $\text{mmol m}^{-2} \text{d}^{-1}$ , and decreased towards the end of the experiment. The range of  $\text{NO}_3^-$  fluxes for the treatments were lower at the end of the experiment (see Fig. S4). Time-integrated  $\text{NO}_3^-$  fluxes were usually positive, close to 0 and without significant differences among treatments (Fig. 3) (Table 1).

#### *$\text{PO}_4^{3-}$*

$\text{PO}_4^{3-}$  fluxes ranged from  $0.18 \pm 0.03$  to  $0.72 \pm 0.09$   $\text{mmol m}^{-2} \text{d}^{-1}$ , and showed idiosyncratic trends during the experiment (see Fig. S4). *Worms* have an effect of increasing time-integrated  $\text{PO}_4^{3-}$  fluxes by 0.21 with a CI of 0.04 to 0.38  $\text{mmol m}^{-2} \text{d}^{-1}$  (Fig. 3) (Table 1).

#### *Organic matter*

OM depth-integrated values ranged from  $0.89 \pm 0.01$  to  $1.09 \pm 0.12\%$  (Fig. 4). In general, the OM concentration in the sediment at the end of the experiment was lower than the initial values. OM depth-integrated values had significant differences between -OM and +OM cores (Table 1).

#### *Fe-sulphide accumulation*

AVS accumulation depth-integrated values ranged from  $32.6 \pm 3.6$  to  $196.0 \pm 31.8$   $\text{mmol m}^{-2}$  (Fig. 1). AVS accumulation was generally higher in most cores in the beginning than at the end of the experiment (Fig. 1). AVS depth-integrated accumulation showed a significant interaction between OM and M (Table 1). The greatest accumulation of AVS

was obtained in +OM–W–M cores ( $196.0 \pm 31.8 \text{ mmol m}^{-2}$ ). +OM–W cores with *shell-hash* (+MS and +MB) had an effect decreasing the AVS accumulation by 97.8 with a CI of 7.0 to  $128.6 \text{ mmol m}^{-2}$  compared to cores without *shell-hash* (-M). The effect of *shell-hash* separated when being in surface (+MS) than when buried (+MB) under *organic pollution* conditions is shown in Fig. 2.

#### *Bioirrigation rates*

Irrigation rates according to Br- inventories were significantly higher in +W cores than –W cores (see Fig. S2), indicating the capacity of bioirrigation of the worms used.

#### **Discussion**

This study shows that under organic pollution, shell-hash can influence sediment metabolism, diminishing the prevalence of anaerobic pathways, and consequently, preventing AVS accumulation and reducing  $\text{NH}_4^+$  release to the water column. This is expected to have a considerable long-lasting effect, and to be more evident in the absence of macrofauna, although in some cases shell-hash and macrofauna can have cumulative effects.

The addition of OM-enhanced sediment led to higher  $\text{TCO}_2$  and SOU fluxes than in unenriched conditions. Ratios between  $\text{TCO}_2$  and SOU fluxes indicated whether the biogeochemical cycling was balanced (ratio close to 1) or alternatively whether the by-products resulting from anaerobic pathways (mainly sulphides) were not re-oxidised, but accumulated in the sediment in the form of AVS (for ratios higher than 1) (Canfield 1989, 1994). Despite the increase in sediment metabolism due to organic pollution, the  $\text{TCO}_2:\text{O}_2$  ratios were comparable between –OM and +OM cores. This indicates that anaerobic pathways were not notably boosted in sediments suffering organic pollution. In the sediments with neither worms nor shell-hash, anaerobic metabolic pathways

seemed to be promoted, because both the  $\text{TCO}_2:\text{O}_2$  ratio and the AVS accumulation increased.

In the absence of worms, AVS accumulation under organic pollution was also relatively high when the shell-hash was just deposited in the surface. This could be because shell-hash positioned horizontally on the surface of the sediment may have hindered the diffusion of solutes (such as  $\text{O}_2$ ) between the water column and the sediment. Nonetheless, AVS accumulation was lower than when no shell-hash was present, and similar to the unenriched conditions with no worms. Both, the  $\text{TCO}_2:\text{O}_2$  ratio and AVS accumulation, decreased when shell-hash was embedded slightly deeper in the stratigraphy of the sediment. This suggests that the effect of shell-hash may be more effective when it is integrated into the sediment stratigraphy, modifying its grain size and thus, increasing its habitat complexity. Accordingly, the effect of shell-hash on the sediment is expected to have a long-lasting effect.

Macrofauna promotes solute exchange between the water column and sediment porewater (Meysman, Middelburg & Heip 2006), as shown by the irrigation rates ( $\text{Br}^-$  content) in our study. This activity had an important role in decreasing the accumulation of by-products derived from sediment metabolism (Aller & Aller 1998; Valdemarsen & Kristensen 2005). When shell-hash and worms acted in combination, the effect was more pronounced, and as when worms were absent, there was a stronger effect when shell-hash was integrated in the sediment stratigraphy than when it was just positioned on the surface. Therefore, the decrease in AVS accumulation is expected to be greater when the habitat complexity of the sediment is maximized by macrofauna and shell-hash.

$\text{NH}_4^+$  release to the water column was impeded by shell-hash under organic pollution, both when worms were present and absent. Macrofauna-induced bioturbation creates microhabitats that favour the coupling between nitrification and denitrification (Gilbert, Bonin & Stora 1995). The increase in habitat complexity caused by shell-hash could promote denitrification, thus explaining the decrease of  $\text{NH}_4^+$  release in sediments under organic pollution and without macrofauna.  $\text{NO}_x$  fluxes were not influenced by shell-hash. The relatively low values of  $\text{NO}_x$  fluxes could be explained by a tight coupling of the nitrification-denitrification pathways (Middelburg *et al.* 1996).

Similarly, shell-hash did not affect  $\text{PO}_4^{3-}$  release, but it was positively affected by worms (Sundby *et al.* 1992). The similarity between different shell-hash treatments could be because the sediment surface was oxidized, demonstrated by the presence of a thin yellowish/lighter layer in the first millimetres of the sediment surface, which was visible in all cores. The oxidized surface controls  $\text{PO}_4^{3-}$  release acting as an “Fe lid”, by keeping the Fe in the ferric form, allowing it to retain a comparable amount of  $\text{PO}_4^{3-}$  in the sediment (Rozan *et al.* 2002). Therefore, changes in  $\text{PO}_4^{3-}$  release could be influenced mainly by changes in the thickness of the oxidized sediment layer in the surface rather than by habitat complexity.

Habitat complexity modulates the structure and function of biological communities, although the mechanisms underlying this relationship remain unclear (Cardinale *et al.* 2002). In this experiment, the structure of shell-hash was expected to increase habitat complexity, leading to the enhancement of aerobic pathways in several aspects. Firstly, an augment in the grain size of the sediment was expected to increase the diffusion rates between the water column and sediment porewater (Bengt-Owe Jansson 1967). Secondly, the roughness and structure of shell-hash can modify the advective porewater flux, favouring the formation of microzones and microlayers



(Huettel & Gust 1992). Thirdly, as shell-hash is a hard surface, it is a suitable habitat for the development of bacteria in biofilms (Gutierrez *et al.* 2003), which are hot-spots of bacteria activity, having an important role in the cycling of elements (Welsh & Castadelli 2004). Increases in habitat complexity created by shell-hash may have resulted in the promotion of benthic aerobic metabolism (Cardinale *et al.* 2002), decreasing the production of by-products derived from organic pollution (Papasprou, Thessalou-Legaki & Kristensen 2010; Kanaya 2014; Martinez-Garcia *et al.* 2015).

The toxicity generated by these by-products can cause the disappearance of macrofauna. In turn, the loss of macrofauna causes a decrease in the active exchange of particles and solutes between porewater and the water column. This results in the erosion of the ecological functions that macrofauna provide, such as the enhancement of sediment metabolic capacity, unbalanced nutrient cycling, etc. This study demonstrates that shell-hash has a positive effect by decreasing the accumulation of toxic by-products derived from organic pollution, and having complementary effects with macrofauna on sulphide. Additionally, shell-hash seems to have similar effects to macrofauna in diminishing the release of  $\text{NH}_4^+$ . This could be explained by the fact that both shell-hash and macrofauna promote the coupling between nitrification and denitrification, thus stimulating the release of  $\text{N}_2$  versus other N forms that are bioavailable for plants and can promote the negative consequences of eutrophication.

Mesocosm experiments are robust ecological approaches that allow us to control environmental variables and therefore to study cause-effects relationships, by testing both the main effects and the interactions between variables. Mesocosms provide important data that cannot be obtained by direct environmental sampling or other research approaches. Nevertheless, extrapolations must be made with care, because mesocosms are simplifications of the natural environment. Consequently, these

Accepted Article

experiments should simulate the natural environmental conditions as closely as possible. In this experiment,  $\text{TCO}_2$ ,  $\text{O}_2$ ,  $\text{NH}_4^+$ ,  $\text{NO}_3^-$ ,  $\text{NO}_2^-$  and  $\text{PO}_4^{3-}$  fluxes as well as AVS accumulation were comparable with *in situ* measurements (Sundby *et al.* 1992; Christensen *et al.* 2000; Callier *et al.* 2006; Giles, Pilditch & Bell 2006). Additionally, the bioirrigation rates were comparable with other studies when using whole macrofauna assemblages (Kristensen & Holmer 2001). Thus, the results obtained in this experiment provide promising insights into the potential use of shell-hash as a tool for mitigating the deleterious effects of organic pollution on soft sediments.

Shell-hash is the main waste product derived from mussel culture. Spain has the second-highest mussel production in the world (between 150 000 and 250 000 T year<sup>-1</sup>), and produces *c.* 80 000 T year<sup>-1</sup> of waste product (APROMAR 2015). Shell-hash debris usually have no intrinsic economic value, and very little is recycled e.g. only 9% in Spain (e.g. only 9% in Spain Consellería de Medio Ambiente de Galicia 2011). Disposal to landfill can be costly (e.g. in the United Kingdom the cost is £80 per tonne; Talbot 2014), leading to illegal dumping events. If shell-hash was used as a tool to mitigate organic pollution in the density proposed in our experiment, it could involve the re-cycling of 1900 tonnes of shell-hash per km<sup>2</sup> of treated seabed.

Although organic pollution is wide-spread in marine sediments, mitigation measures are rarely implemented. The addition of shell-hash to the sediment is not expected to be particularly costly because it could be deployed from the water surface. The integration of shell-hash into the stratigraphy of the sediment would occur naturally, without any requirement for mechanical intervention. Nevertheless, a cost-benefit analysis would be necessary to establish the most suitable method to transfer shell-hash to the sediment in order to minimize costs and the carbon footprint.

In some cases, sediments that are subjected to shell-hash deposition, such as the ones influenced by mussel culture, have been dredged to remove mussel shells from the sediment. Our results suggest that it may be better not to dredge these areas, at least if the density of shell-hash is similar to the one used in this study. This measure would be beneficial for sediment biogeochemical processes, and would reduce the carbon footprint derived from dredging.

This study demonstrates that under conditions of organic pollution, shell-hash can reduce the accumulation of by-products from anaerobic metabolic pathways, improving the sediment's ecological status. Shell-hash can decrease the release rate of ammonium to the water column, thus preventing the negative ecological consequences derived from eutrophication. Therefore, shell-hash debris derived as a 'waste-product' of anthropogenic activities could be used to mitigate the effects of organic pollution on marine sediments, particularly in defaunated sites.

### **Acknowledgments**

We are grateful to Ginés García García for his advice and help with the collection of the polychaetes, and to José Vicente Guardiola Bartolomé for kindly providing the pH meter and oxymeter. We would also like to thank Felipe Aguado-Gimenez for providing the incubation system, and the technicians of the Marine Science laboratory at the University of Alicante for their help during the analyses. We also appreciate the comments of two anonymous reviewers, which have improved the manuscript. This work has been funded by the project GRE14-19 from the University of Alicante, the project GV/2015/001 from the "Conselleria de Educación, Cultura y Deporte" of the government of the Valencia region, the national project CGL2015-70136-R (MINECO/FEDER) and the contract and "Juan de la Cierva" (ref. JCI-2012-12413)

This article is protected by copyright. All rights reserved.

from the Ministerio de Economía y Competitividad of Spain to CS.

### Data accessibility

All data used in this paper are archived in Dryad Digital Repository

<http://dx.doi.org/10.5061/dryad.kj51b> (Casado-Coy *et al.* 2016).

### References

Allen, H.E., Fu, G. & Deng, B. (1993) Analysis of acid-volatile sulfide (AVS) and simultaneously extracted metals (SEM) for the estimation of potential toxicity in aquatic sediments. *Environmental Toxicology and Chemistry*, **12**, 1441–1453.

Aller, R.C. & Aller, J.Y. (1998) The effect of biogenic irrigation intensity and solute exchange on diagenetic reaction rates in marine sediments. *Journal of Marine Research*, **56**, 905–936.

APROMAR. (2015) *La Acuicultura En España 2015*.

Barros, M.C., Bello, P.M., Bao, M. & Torrado, J.J. (2009) From waste to commodity: transforming shells into high purity calcium carbonate. *Journal of Cleaner Production*, **17**, 400–407.

Bengt-Owe Jansson. (1967) The significance of grain size and pore water content for the interstitial fauna of sandy beaches. *Oikos*, **2**, 311–322.

Callier, M.D., Weise, A.M., McKindsey, C.W. & Desrosiers, G. (2006) Sedimentation rates in a suspended mussel farm (Great-Entry Lagoon, Canada): Biodeposit

production and dispersion. *Marine Ecology Progress Series*, **322**, 129–141.

Canfield, D.E. (1989) Reactive iron in marine sediments. *Geochimica et Cosmochimica Acta*, **53**, 619–632.

Canfield, D.E. (1994) Factors influencing organic carbon preservation in marine sediments. *Chemical Geology*, **114**, 315–329.

Cardinale, B.J., Palmer, M.A., Swan, C.M., Brooks, S. & LeRoy Poff, N. (2002) The influence of substrate heterogeneity on biofilm metabolism in a stream ecosystem. *Ecology*, **83**, 412–422.

Casado-Coy, N., Martinez-Garcia, E., Sanchez-Jerez, P. & Sanz-Lazaro, C. (2016) Data from: Mollusc-shell debris can mitigate the deleterious effects of organic pollution on marine sediments. Dryad Digital Repository, <http://dx.doi.org/10.5061/dryad.kj51b>

Christensen, P.B., Rysgaard, S., Sloth, N.P., Dalsgaard, T. & Schw??rter, S. (2000) Sediment mineralization, nutrient fluxes, denitrification and dissimilatory nitrate reduction to ammonium in an estuarine fjord with sea cage trout farms. *Aquatic Microbial Ecology*, **21**, 73–84.

Cloern, J.E. (2001) Our evolving conceptual model of the coastal eutrophication problem. *Marine Ecology Progress Series*, **210**, 223–253.

Consellería de Medio Ambiente de Galicia. (2011) *Plan de Xestión de Residuos Industriais E Solos Contaminados de Galicia*. Spain.

Dolmer, P. & Frandsen, R.P. (2002) Evaluation of the Danish mussel fishery: Suggestions for an ecosystem management approach. *Helgoland Marine Research*,

56, 13–20.

Duarte, C.M., Middelburg, J.J. & Caraco, N. (2005) Major role of marine vegetation on the oceanic carbon cycle. *Biogeosciences*, **2**, 1–8.

Gilbert, F., Bonin, P. & Stora, G. (1995) Effect of bioturbation on denitrification in a marine sediment from the West Mediterranean littoral. *Hydrobiologia*, **304**, 49–58.

Giles, H., Pilditch, C.A. & Bell, D.G. (2006) Sedimentation from mussel (*Perna canaliculus*) culture in the Firth of Thames, New Zealand: Impacts on sediment oxygen and nutrient fluxes. *Aquaculture*, **261**, 125–140.

Glud, R.N. (2008) Oxygen dynamics of marine sediments. *Marine Biology Research*, **4**, 243–289.

Gran, G., Dahlenborg, H., Laurell, S. & Rottenberg, M. (1950) Determination of the Equivalent Point in Potentiometric Titrations. *Acta Chemica Scandinavica*, **4**, 559–577.

Gray, J.S., Wu, R.S. & Or, Y.Y. (2002) Effects of hypoxia and organic enrichment on the coastal marine environment. *Marine Ecology Progress Series*, **238**, 249–279.

Gutierrez, J.L., Jones, C.G., Strayer, D.L. & Iribarne, O.O. (2003) Mollusks as ecosystem engineers: the role of shell production in aquatic habitats. *Oikos*, **101**, 79–90.

Hargrave, B.T., Holmer, M. & Newcombe, C.P. (2008) Towards a classification of organic enrichment in marine sediments based on biogeochemical indicators. *Marine Pollution Bulletin*, **56**, 810–824.

Heilskov, A.C., Alperin, M. & Holmer, M. (2006) Benthic fauna bio-irrigation effects

on nutrient regeneration in fish farm sediments. *Journal of Experimental Marine Biology and Ecology*, **339**, 204–225.

Holmer, M. & Barry, W. (2005) Organic enrichment from marine finfish aquaculture and effects on sediment biogeochemical processes. *Handbook of Environmental Chemistry* pp. 181–206.

Holmer, M., Duarte, C.M. & Marbá, N. (2005) Iron additions reduce sulfate reduction rates and improve seagrass growth on organic-enriched carbonate sediments. *Ecosystems*, **8**, 721–730.

Holmer, M., Marba, N., Diaz-Almela, E., Duarte, C.M., Tsapakis, M. & Danovaro, R. (2007) Sedimentation of organic matter from fish farms in oligotrophic Mediterranean assessed through bulk and stable isotope ( $^{13}\text{C}$  and  $^{15}\text{N}$ ) analyses. *Aquaculture*, **262**, 268–280.

Huettel, M. & Gust, G. (1992) Impact of bioturbation on interfacial solute exchange in permeable sediments. *Marine Ecology Progress Series*, **89**, 253–267.

Islam, M.S. & Tanaka, M. (2004) Impacts of pollution on coastal and marine ecosystems including coastal and marine fisheries and approach for management: A review and synthesis. *Marine Pollution Bulletin*, **48**, 624–649.

John I. Hedge, R.G.K. (1995) Sedimentary organic matter preservation: an assessment and speculative synthesis. *Marine chemistry*, **49**, 137–139.

Jørgensen, B.B. (1982) Mineralization of organic matter in the sea bed - the role of sulphide reduction. *Nature*, **296**, 643–645.

Kanaya, G. (2014) Recolonization of macrozoobenthos on defaunated sediments in a

hypertrophic brackish lagoon: Effects of sulfide removal and sediment grain size. *Marine Environmental Research*, **95**, 81–88.

Kristensen, E. & Holmer, M. (2001) Decomposition of plant materials in marine sediment exposed to different electron acceptors (O<sub>2</sub>, NO<sub>3</sub> and SO<sub>4</sub><sup>2-</sup>), with emphasis on substrate origin, degradation kinetics, and the role of bioturbation. *Geochimica et Cosmochimica Acta*, **65**, 419–433.

Martinez-Garcia, E., Carlsson, M.S., Sanchez-Jerez, P., Sánchez-Lizaso, J.L., Sanz-Lazaro, C. & Holmer, M. (2015) Effect of sediment grain size and bioturbation on decomposition of organic matter from aquaculture. *Biogeochemistry*, **125**, 133–148.

McManus, J.W. (1997) Tropical marine fisheries and the future of coral reefs: a brief review with emphasis on Southeast Asia. *Coral Reefs*, **16**, S121–S127.

Meysman, F.J.R., Middelburg, J.J. & Heip, C.H.R. (2006) Bioturbation: a fresh look at Darwin's last idea. *Trends in Ecology and Evolution*, **21**, 688–695.

Middelburg, J.J., Soetaert, K., Herman, P.M.J. & Heip, C.H.R. (1996) Denitrification in marine sediments: A model study. *Global Biogeochemical Cycles*, **10**, 661–673.

Morrisey, D.J., Gibbs, M.M., Pickmere, S.E. & Cole, R.G. (2000) Predicting impacts and recovery of marine-farm sites in Stewart Island, New Zealand, from the Findlay-Watling model. *Aquaculture*, **185**, 257–271.

Nakagawa, S. & Cuthill, I.C. (2007) Effect size, confidence interval and statistical significance: A practical guide for biologists. *Biological Reviews*, **82**, 591–605.

Newell, R.I.E. (2004) Ecosystem influences of natural and cultivated populations of



suspension-feeding bivalve molluscs: a review. *Journal of Shellfish Research*, **23**, 51–61.

Papaspyrou, S., Thessalou-Legaki, M. & Kristensen, E. (2010) The influence of infaunal (*Nereis diversicolor*) abundance on degradation of organic matter in sandy sediments. *Journal of Experimental Marine Biology and Ecology*, **393**, 148–157.

Pearson, T.H. & Rosenberg, R. (1978) Macrobenthic succession in relation to organic enrichment and pollution of the marine environment. *Oceanography and marine biology annual review*, **16**, 229–311.

Piedecausa, M.A., Aguado-Giménez, F., Cerezo Valverde, J., Hernández Llorente, M.D. & García-García, B. (2012) Influence of fish food and faecal pellets on short-term oxygen uptake, ammonium flux and acid volatile sulphide accumulation in sediments impacted by fish farming and non-impacted sediments. *Aquaculture Research*, **43**, 66–74.

Rozan, T.F., Taillefert, M., Trouwborst, R.E., Glazer, B.T., Ma, S., Herszage, J., Valdes, L.M., Price, K.S. & Iii, G.W.L. (2002) Iron-sulfur-phosphorus cycling in the sediments of a shallow coastal bay: Implications for sediment nutrient release and benthic macroalgal blooms. *Limnology and Oceanography*, **47**, 1346–1354.

Sanz-Lazaro, C., Belando, M.D., Marin-Guirao, L., Navarrete-Mier, F. & Marin, A. (2011) Relationship between sedimentation rates and benthic impact on Ma??rl beds derived from fish farming in the Mediterranean. *Marine Environmental Research*, **71**, 22–30.

Sanz-Lázaro, C. & Marín, A. (2008) Assessment of Finfish Aquaculture Impact on the Benthic Communities in the Mediterranean Sea. *Dynamic Biochemistry, Process*

*Biotechnology and Molecular Biology*, **2**, 21–32.

Sanz-Lazaro, C., Valdemarsen, T. & Holmer, M. (2015) Effects of temperature and organic pollution on nutrient cycling in marine sediments. *Biogeosciences*, **12**, 4565–4575.

Sanz-Lázaro, C., Valdemarsen, T., Marín, A. & Holmer, M. (2011) Effect of temperature on biogeochemistry of marine organic-enriched systems: Implications in a global warming scenario. *Ecological Applications*, **21**, 2664–2677.

Sebens, K.P. (1991) Habitat structure and community dynamics in marine benthic systems. *Habitat Structure*, **1st**, 211–234.

Stief, P. (2013) Stimulation of microbial nitrogen cycling in aquatic ecosystems by benthic macrofauna: Mechanisms and environmental implications. *Biogeosciences*, **10**, 7829–7846.

Sundby, B., Gobeil, C., Silverberg, N. & Mucci, A. (1992) The phosphorus cycle in coastal marine sediments. *Limnology and Oceanography*, **37**, 1129–1145.

Talbot, A. (2014) *Qualitative Research into Drivers of Diversion from Landfill and Innovation in the Waste Management Industry*. UK.

Underwood, A.J. (1997) Experiments in Ecology: Their logical design and interpretation using analysis of variance. *University of Cambridge*, 1–522.

Valdemarsen, T. & Kristensen, E. (2005) Diffusion scale dependent change in anaerobic carbon and nitrogen mineralization: True effect or experimental artifact? *Journal of Marine Research*, **63**, 645–669.

Valdemarsen, T., Kristensen, E. & Holmer, M. (2010) Sulfur, carbon, and nitrogen

cycling in faunated marine sediments impacted by repeated organic enrichment.

*Marine Ecology Progress Series*, **400**, 37–53.

Welsh, D.T. & Castadelli, G. (2004) Bacterial nitrification activity directly associated with isolated benthic marine animals. *Marine Biology*, **144**, 1029–1037.

Wentworth, C.K. (1922) A SCALE OF GRADE AND CLASS TERMS FOR CLASTIC SEDIMENTS' CHESTER. *The Journal of Geology*, **30**, 377–392.

Wilding, T.A. (2012) Changes in Sedimentary Redox Associated with Mussel (*Mytilus edulis* L.) Farms on the West-Coast of Scotland. *PLoS ONE*, **7**.

### Supporting Information

Additional Supporting Information may be found in the online version of this article:

Table S1. Summary of the Student-Newman-Keuls *post-hoc* tests based on the significant interactions among factors in the ANOVA for the response variables shown in Table 1.

Fig. S1. A) Approximate amount of *shell-hash* added in the cores, which corresponded to c. 5.4 gr. B) Photographs of shell-hash position in the cores.

Fig. S2. Irrigation rates of the sediment ( $\text{Br}^-$  content), depth-integrated (0–16cm).

Fig. S3. Trends of SOU and of total  $\text{CO}_2$  ( $\text{TCO}_2$ ),  $\text{NH}_4^+$  fluxes during the experiment.

Fig. S4. Trends of  $\text{NO}_3^-$ ,  $\text{NO}_2^-$  and  $\text{PO}_4^{3-}$  fluxes during the experiment.

## Tables and Figures

Table 1. Results of the ANOVA for the time-integrated fluxes of total CO<sub>2</sub> (TCO<sub>2</sub>), SOU, NH<sub>4</sub><sup>+</sup>, NO<sub>3</sub><sup>-</sup>, NO<sub>2</sub><sup>-</sup>, PO<sub>4</sub><sup>3-</sup>, depth-integrated acid volatile sulphide (AVS) and organic matter percentage (OM%) at the end of the experiment. The factors were *organic pollution* (OM), *worm* (W) and *shell-hash* (M). Significant effects are indicated in bold

		SOU			TCO <sub>2</sub>			TCO <sub>2</sub> :O <sub>2</sub>			NH <sub>4</sub> <sup>+</sup>		
Source of variation	df	MS	F	P	MS	F	P	MS	F	P	MS	F	P
OM	1	10024	49.715	< <b>0.001</b>	102575	58.106	< <b>0.001</b>	0.005462	9.019	< <b>0.01</b>	840.9	85.128	< <b>0.001</b>
W	1	1223	6.068	< <b>0.05</b>	723	0.410	> 0.5	0.002436	4.022	> 0.05	93.4	9.451	< <b>0.01</b>
M	2	405	2.009	> 0.1	1446	0.819	> 0.4	0.001789	2.954	> 0.07	26.4	2.669	> 0.08
OM x W	1	66	0.326	> 0.5	6592	3.734	> 0.06	0.006357	10.496	< <b>0.01</b>	13.1	1.323	> 0.2
OM x M	1	806	3.997	< <b>0.05</b>	16099	9.120	< <b>0.01</b>	0.007190	11.871	< <b>0.001</b>	49.5	5.009	< <b>0.05</b>
W x M	1	293	1.451	> 0.2	7892	4.471	< <b>0.05</b>	0.000178	0.294	> 0.7	65.6	6.640	< <b>0.01</b>
OM x W x M	1	56	0.280	> 0.7	8053	4.562	< <b>0.05</b>	0.004812	7.945	< <b>0.01</b>	8.9	0.904	> 0.4
Residual	16	202			1765			0.000606			9.9		
Total	23												
Cochran's C test		C=0.445, P<0.05			C=0.2798, P>0.05			C=0.38162, P>0.05			C=0.2292, P>0.05		
Transformation		none			none			none			none		
		NO <sub>3</sub> <sup>-</sup>			NO <sub>2</sub> <sup>-</sup>			PO <sub>4</sub> <sup>3-</sup>			%OM		
Source of variation	df	MS	F	P	MS	F	P	MS	F	P	MS	F	P
OM	1	0.016886	1.422	> 0.2	0.10366	19.175	< <b>0.001</b>	0.0012	0.054	> 0.8	0.08316	6.934	< <b>0.05</b>
W	1	0.014150	1.192	> 0.2	0.00062	0.115	> 0.7	0.3973	18.507	< <b>0.001</b>	0.01341	1.118	> 0.3
M	1	0.015055	1.268	> 0.3	0.00202	0.373	> 0.6	0.0350	1.632	> 0.2	0.00400	0.334	> 0.7
OM x W	1	0.008033	0.676	> 0.4	0.00109	0.201	> 0.6	0.0600	2.795	> 0.1	0.01733	1.445	> 0.2
OM x M	1	0.003998	0.337	> 0.7	0.00046	0.085	> 0.9	0.0972	4.528	< <b>0.05</b>	0.01080	0.900	> 0.4
W x M	1	0.008307	0.700	> 0.5	0.00124	0.229	> 0.7	0.0426	1.986	> 0.1	0.00109	0.091	> 0.9
OM x W x M	1	0.004610	0.388	> 0.6	0.00016	0.030	> 0.9	0.0107	0.499	> 0.6	0.00448	0.374	> 0.6
Residual	16	0.011875			0.00541			0.0215			0.01199		
Total	23												
Cochran's C test		C= 0.2466, P>0.05			C=0.5228, P<0.05			C=0.3659, P>0.05			C=0.3452, P>0.05		
Transformation		none			none			none			none		

### AVS

Source of variation	df	MS	F	P
OM	1	3376	5.726	< <b>0.05</b>
W	1	18168	30.809	< <b>0.001</b>
M	1	2982	5.057	< <b>0.05</b>
OM x W	1	279	0.473	> 0.4
OM x M	1	3453	5.856	< <b>0.01</b>
W x M	1	765	1.297	> 0.2
OM x W x M	1	461	0.782	> 0.4
Residual	16	590		
Total	23			
Cochran's C test			C=0.4296, P<0.05	
Transformation			none	

Figure 1. Time-integrated fluxes of total CO<sub>2</sub> (TCO<sub>2</sub>) (A), SO<sub>4</sub><sup>2-</sup> (SOU) (B), TCO<sub>2</sub> and O<sub>2</sub> integrated fluxes ratio (C) and depth-integrated acid volatile sulphide (AVS) at the end of the experiment (D) (n=3, mean ± SE). See legend of Table 1 for the abbreviations of each treatment.

Figure 2. Effect size (with a CI of variables) of the effect of the *shell-hash* factor in organic pollution conditions in time-integrated fluxes of TCO<sub>2</sub> (A), NH<sub>4</sub><sup>+</sup> (B) and depth-integrated acid volatile sulphide (AVS) at the end of the experiment (C). See legend of Table 1 for the abbreviations of each treatment.

Figure 3. Time-integrated fluxes of NH<sub>4</sub><sup>+</sup> (A), PO<sub>4</sub><sup>3-</sup> (B), NO<sub>3</sub><sup>-</sup> (C) and NO<sub>2</sub><sup>-</sup> (D) (n=3, mean ± SE). See legend of Table 1 for the abbreviations of each treatment.

Figure 4. Depth-integrated (0 – 16 cm) organic matter percentage (OM%) (n=3, mean ± SE). See legend of Table 1 for the abbreviations of each treatment.

Figure 1.

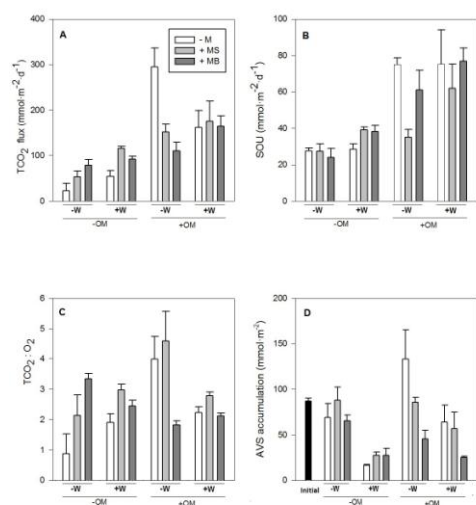


Figure 2

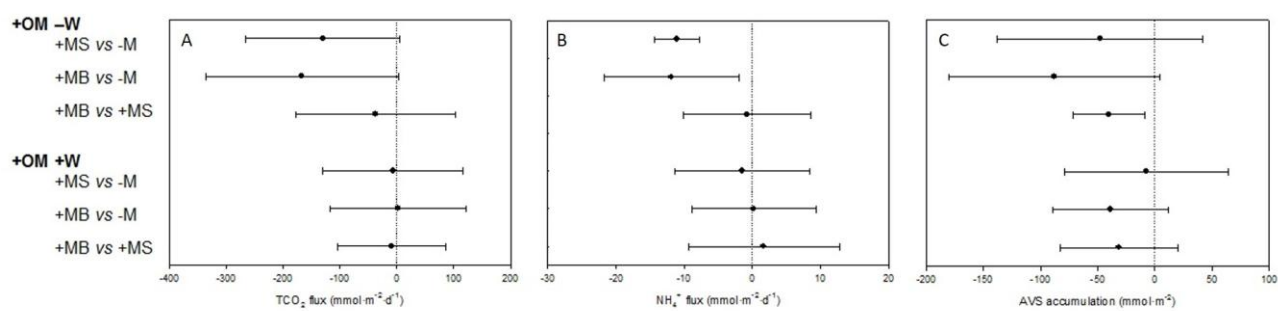


Figure 3.

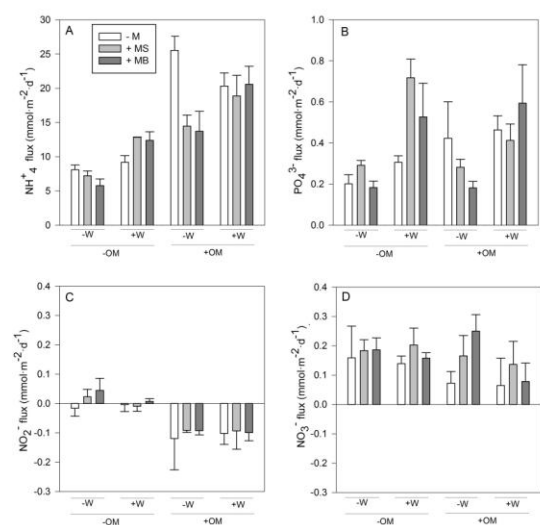


Figure 4.

